https://dx.doi.org/10.1016/j.nanoen.2021.106272

Wearable self-powered human motion sensors based on highly stretchable quasi-solid state hydrogel

Jianhao Chen[a], Lei Zhang[b*], Yingyi Tu[a], Qiao Zhang[a*], Feng Peng[a], Wei Zeng[b*], Mingqiu Zhang[c], Xiaoming Tao[d]

[a] School of Chemistry and Chemical Engineering, Guangzhou University, Guangzhou 510006, China

[b] Department of flexible sensing technology, Institute of Chemical Engineering, Guangdong Academy of Sciences, Guangzhou 510665, China

[c] Key Laboratory for Polymeric Composite and Functional Materials of Ministry of Education, GD HPPC Lab, School of Chemistry and Chemical Engineering, Sun Yat-Sen University, Guangzhou 510275, P. R. China

[d] Research Centre for Smart Wearable Systems, Institute of Textiles and Clothing, The Hong Kong Polytechnic University, Hong Kong

* Corresponding authors:

zengwei@gdcri.com (Wei Zeng)

zhangqiao@gzhu.edu.cn (Qiao Zhang)

zhanglei@gdcri.com (Lei Zhang)

https://dx.doi.org/10.1016/j.nanoen.2021.106272

ABSTRACT

Self-powered flexible sensors are highly favored and considered auspicious for wearable electronics due to their preferable flexibility and facilitation to integrate with various apparel products. As a wearable product, the sensors can be designed by a self-powered strategy powered with harvested low-grade heat from human body to meet the daily long-term use. The flexible thermoelectric generator (f-TEG) can harvest the human body heat to generate a thermovoltage driving the sensor directly. Herewith we report a wearable self-powered human motion sensor made from highly stretchable quasi-solid state hydrogel, which shows 2800% elongation at break and good strain sensitivity (GF=4, when the strain is 200%) and detects the movement and sound of human body. Further, the hydrogel based sensor can harvest the human body heat and generate a thermovoltage to drive the sensor directly, which exhibits an impressive gigantic Seebeck coefficient of approximate 11.5 mV K^{-1} at ambient temperature. Combining the merits of flexibility, environment friendly, sensitivity and thermoelectric performance at room temperature range together, we believe that the hydrogel based sensor will offer amble opportunities to numerous self-powered sensor applications like wearable electronics, sports, health and wellbeing.

Keywords: self-powered, flexible sensors, quasi-solid state hydrogel, thermoelectric generator, body heat,

https://dx.doi.org/10.1016/j.nanoen.2021.106272

Introduction

Wearable electronic devices have attracted more and more attention due to their flexibility, portability and biocompatibility, which can be applied to electronic skin, health monitoring, artificial intelligence, soft robots[1-6]. As the core component of wearable electronic devices, stress or strain-based sensors are rapidly designed to continuously monitor human activities, heartbeat and pulse. Such sensors change mechanical motion into detectable signals[7-9]. However, traditional sensors are made of stiff materials, such as silicon, metals, semiconductors, etc., which do not have high tensile properties[10-15]. Meanwhile, these battery-powered sensors need to be recharged frequently, which is not ideal for monitoring human activity over long periods of time. Self-powered sensors can be developed to allow sensors to work for long periods of time without additional power[16, 17]. Therefore, developing a flexible self-powered sensor will provide greater feasibility for wearable devices to be used for human movement and health monitoring.

For the development of self-powered flexible sensors, great efforts have been concentrated on flexible nanogenerators (NGs)[18, 19], triboelectric nanogenerators (TENGs)[20, 21], piezoelectric nanogenerator (PENGs)[22, 23], flexible solar cells[24], which may directly harvest energy from the surroundings. Although solar energy is abundant, solar cells are always limited under different environmental conditions. Similarly, vibration-based energy collectors are limited by body movement. Thermoelectric generators (TEGs) based on Seebeck effect is plausible for harvesting low-grade heat which can produce electric energy for the use of sensors through the

https://dx.doi.org/10.1016/j.nanoen.2021.106272

temperature difference between human body and surrounding[25]. Nevertheless, commonly used thermoelectric materials are metal complexes or alloys and TEGS made of these materials are usually rigid and have poor tensile properties, which is not conducive to the use of wearable devices[26]. Until recently, increasing interest in uniquely designed hydrogel with ionic conductive property is being gained by inter-disciplinary fields compared to traditional ones in terms of softness, wearability, flexibility, and customization ability.[27]. For instance, a dual conductive percolation network hydrogel strain sensor has been designed by Han's group, which exhibits high conductivity, anti-freezing and self-healing[28]. In addition to conductivity, sensitivity and sensing performance are crucial for the hydrogel sensor. Zhang et al. has fabricated hydrogel composites incorporating MXene ($Ti_3C_2T_x$) that exhibits great sensitivity with a gauge factor of 25 and outstanding performance in advanced sensing applications[29]. However, these ionic conductive hydrogel sensors are lack of the ability of self-powering, making it difficult to operate in electronic devices for a long time.

Combining the merits of thermoelectric voltage and sensitivity of ionic conductive hydrogel, the hydrogel based thermoelectric generator is suitable for self-powered wearable strain sensor. Similar to the Seebeck effect of conductor, semiconductor, or conductive polymer which electronic charge carriers will migrate from the hot side to the cold side and accumulate at the cold end to generate a thermoelectric voltage, Soret effect is the result of thermo-diffusion of ions in the solid electrolyte. Since ions cannot pass through the electrode, they can only accumulate at both sides of the electrode. The accumulation of net charge of ions at different electrodes generates thermoelectric

https://dx.doi.org/10.1016/j.nanoen.2021.106272

voltage in the presence of a temperature gradient[30-32]. Therefore, ionic conductive hydrogel based thermoelectric generator can be used for the preparation of self-powered sensors.

Herein, we demonstrate a self-powered wearable strain sensor utilizing dual network hydrogel, which possess a great sensitivity and high thermoelectric voltage. The ion-conductive hydrogel is fabricated by employing polyacrylamide (PAAm) as the first crosslinked network and calcium-alginate (CA) as the second one, Li_2SO_4 as an ion-conductive material and water/glycerol as a dispersion medium. The as-prepared highly stretchable quasi-solid state hydrogel not only shows excellent sensing properties with monitoring capabilities for human activities, also can convert low-grade thermal energy to electricity for self-power sensor with a Seebeck coefficient of up to 11.5mV K^{-1} and an impressive ZT value of 0.087.

Results and discussion

The dual network ion-conductive hydrogel with high tensile properties, great sensitivity and excellent thermoelectric properties was prepared by a two-step method. Acrylamide (AAm) and calcium alginate (CA) were selected as network structures. The fabrication of the Li_2SO_4/polyacrylamide/calcium-alginate (Li_2SO_4/PAAm/CA) is schematically illustrated in Figure 1. First, AAm monomer, cross-linking agent MBAA, thermal initiator KPS and accelerator TEMED were added into the mixed solvent of hydrated glycerin, and then the network structure was formed by chemical cross-linking. Sodium alginate (SA) will be entangled with PAAm in a semi-interpenetrating network structure during cross-linking processing. Glycerin as a solvent added into the hydrogel

https://dx.doi.org/10.1016/j.nanoen.2021.106272

can increase the antifreeze and antiwater loss of hydrogel. In order to further improve the mechanical properties of hydrogels, SA is cross-linked with polyvalent ionic calcium chloride by means of physical crosslinking due to the presence of carboxyl groups in sodium alginate. The ionic bond formed between carboxyl groups in PAAm and calcium ions is dynamic. In addition, hydroxyl groups in glycerol form hydrogen bonds with imino groups in PAAm. Hence, the ion-conductive hydrogel with double interpenetrating network (DN) Li_2SO_4/PAAm/CA has excellent mechanical properties profit from the cooperation of various bonds within hydrogel.

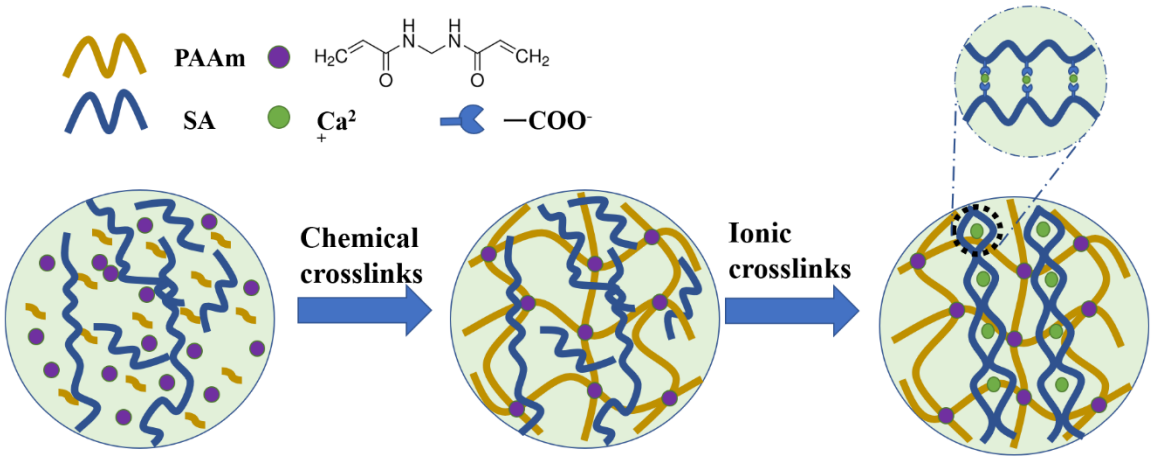

Figure 1. Schematic of the preparation process and chemical structure of the ion-conductive hydrogel.

The ion-conductive hydrogel is essentially a capacitive thermoelectric generator, because the thermally diffused ions cannot be transmitted through the surface of the electrode and can only accumulate at both sides of the electrode to generate a thermoelectric voltage. Therefore, the thermoelectric effect of ion-conductive hydrogel is investigated as a self-powered strategy for the hydrogel based sensor. The working

https://dx.doi.org/10.1016/j.nanoen.2021.106272

mechanism of the ion-conductive hydrogel based thermoelectric generator is shown in Fig. 2a. When there is a temperature difference at both sides of the ion-conductive hydrogel, lithium ions and sulfate ions will migrate from the hot side to the cold side due to the thermo-diffusion effect. In a polymer network structure with high crosslinking density, the migration resistance of lithium ions is less than sulfate ions and lithium ions have a faster migration rate due to the smaller size of lithium ions compared sulfate ions. In addition, due to the existence of Manning condensation, some lithium ions will form agglomeration in the negatively charged polymer chain, which further increases the frictional resistance of sulfate ions. As the distance between ions is larger than the Debye length, eventually lithium ions will accumulate at the cold side and sulfate ions will remain at the hot side, thus generating a thermoelectric voltage. During the discharge process, the two sides of the ion-conductive hydrogel are connected in series through an external circuit, and electrons will flow from the hot side to the cold side. This flow of net charge will cause a decrease in the electric field in the hydrogel and thus a decrease in voltage. When the external circuit is disconnected and the hydrogel is in the open circuit state again, the ion concentration difference is re-established due to the existence of temperature difference, so the voltage will be restored after a period of time. In order to confirm that there is no thermogalvanic effect in the ion-conductive hydrogel, a CV scan have been performed and it can be seen there is no redox peak, indicating that the thermal voltage is caused by the Soret effect (Fig. S1).

https://dx.doi.org/10.1016/j.nanoen.2021.106272

Fig.2b depicts that the output voltage of the ion-conductive hydrogel based thermoelectric generator (Cylinder structure with 15 mm high and 15mm in diameter) is 450 mV under the temperature difference of 40 ºC, when maintain the cold side temperature at 0 ºC and the hot side temperature at 40 ºC. After 50 minutes of thermal charging, the thermal voltage reaches a stable value of 450 mV. The long-term stability of open circuit voltage is also an important indicator, which can show whether our open circuit voltage can be maintained at a stable level. As shown in Fig.S2, the open circuit voltage shows small fluctuate around saturated open circuit voltage when the temperature difference is existed and maintains at least 20 hours. In order to obtain the Seebeck coefficient of the ion-conductive hydrogel based thermoelectric generator, the open circuit voltage of the thermoelectric generator under different temperature differences are measured. The open-circuit voltage increases linearly with the increase of the applied temperature difference, and the slope obtained by fitting these points is the corresponding Seebeck coefficient of 11.5 $mV \cdot K^{-1}$ (Fig. 2c). Furthermore, the output power of the ion-conductive hydrogel based thermoelectric generator also has been investigated as shown in Fig. 2d, the thermoelectric generator produces short-circuit current density as large as 0.42 and 0.84 $A \cdot m^{-2}$ under the temperature difference ($\triangle T$) of 20 ºC and 40 ºC, respectively, which correspond the maximum power density of 23.57 and 94.38 $mW \cdot m^{-2}$. In addition，the thickness of thermoelectric generator would not affected the output thermal voltage, Fig. S3 shows the output thermal voltage of 1 cm thickness is the same as that of 1.5 cm which just depend on the temperature difference between the hot and cold side of the ion-conductive hydrogel based

https://dx.doi.org/10.1016/j.nanoen.2021.106272

thermoelectric generator effect of thickness on thermoelectric properties have been considered. Even the influence of sample thickness on thermoelectric performance could be excluded, the power density of the system would increase with the increase of the thickness under the premise of constant contact area. Hence the effect of thickness can be ignored in this work and the corresponding volume power densities of 1.0 cm and 1.5 cm are 2.357 $W \cdot m^{-3}$ and 1.560 $W \cdot m^{-3}$, respectively.

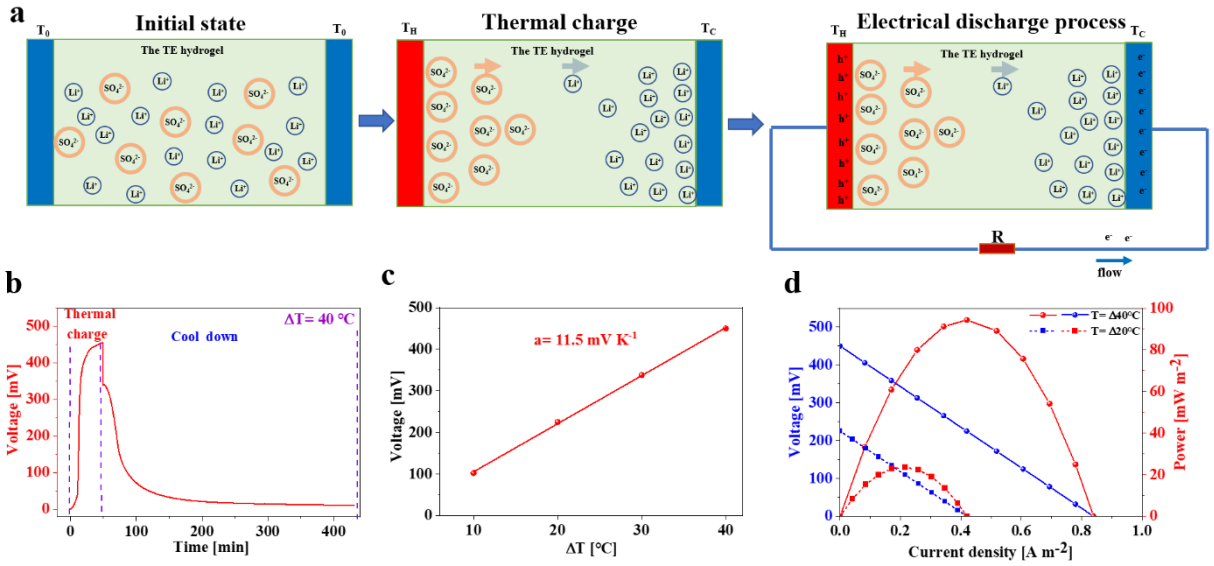

Figure 2. (a) Mechanism of thermal voltage generated by the ion-conductive hydrogel based thermoelectric generator under temperature difference. (b) The output open voltage of the ion-conductive hydrogel under 40 °C temperature difference and cooling down. (c) Dependence of the thermal voltage for the ion-conductive hydrogel on the temperature difference from 10 to 40 °C. (d) Voltage-current density and power density-current density curves under a temperature difference of 20 °C and 40 °C, respectively.

To further characterize the thermoelectric properties of the ion-conductive hydrogel, the ionic conductivity of the ion-conductive hydrogel is measured by AC impedance spectroscopy. Fig. 3a and Fig. S4 reveal that there is no half circle in the

https://dx.doi.org/10.1016/j.nanoen.2021.106272

high-frequency region of the Nyquist plots, which is consistent with the related results of the solid ion gel and gel polymer electrolyte reported previously [32, 33]. The main reason for this phenomenon is the small dielectric relaxation time of the ions in the ion-conductive hydrogel, as a result, the minor capacitance effect on the EIS spectrum. Ionic resistance is obtained by intercepting a straight line along the real axis. According to the EIS spectrum in the temperature range of 25°C to 50°C, the ionic conductivity range of the corresponding temperature is 6.24 to 10.72 $mS \cdot cm^{-1}$ (Fig. 3b). The power factor ($PF = S^2 \sigma$) of the thermoelectric generator is presented in Fig. 3c, the power factor increases significantly from 82.59 to 141.86 $\mu W \cdot m^{-1} \cdot K^{-2}$ when the temperature increases from 20 °C to 50 °C, due to the strong temperature-dependence of S and σ of the ion-conductive hydrogel.

Due to the low thermal conductivity of the hydrogel, it could improve the thermoelectric conversion effectively. The thermal conductivity at different temperatures was measured by the transient plane heat source method. As shown in Fig. 3d, the thermal conductivity of the ion-conductive hydrogel increases from 0.5085 to 0.5264 $W\ m^{-1}k^{-1}$ with the increase of temperature in the range from 25 °C to 50 °C. Further, the ZT value of the ion-conductive hydrogel is 0.048 to 0.087 in the range of 25 °C to 50 °C calculated from the equation of $ZT = T S^2 \sigma/K$ (Fig. 3e). According to our knowledge, in the research of self-powered hydrogel sensors using thermoelectric generators, this ZT value is relatively superior[34, 35]. In order to prove that our ion-conductive hydrogel is not a disposable thermoelectric generator, a cyclic charge-discharge test within a certain period of time have been carried out. As shown in Fig.

https://dx.doi.org/10.1016/j.nanoen.2021.106272

3f, we maintain the cold side temperature at 2°C and the hot side temperature at 38°C. The ion-conductive hydrogel was stabilized at its maximum output voltage by thermal charging for a long time. And then connect the ion-conductive hydrogel to an external circuit and the voltage will change to 0 V within a few seconds. The maximum output voltage of the ion-conductive hydrogel will decrease to a certain extent as the quasi-continuous cycle number increased. This phenomenon may be caused by the polarization of the electrode and there have been similar reports before[36].

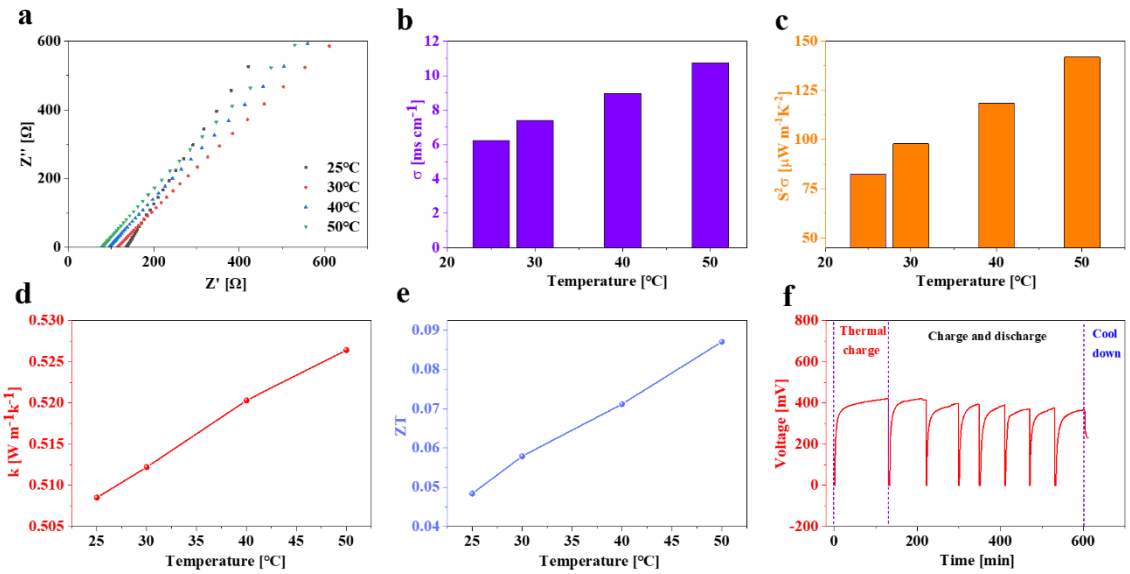

Figure 3. The ion-conductive hydrogel (a) The Nyquist plots under 20 to 50°C. (b) Ion conductivity. (c) Power factor. (d) Thermal conductivity. (e) The figure of merit. (f) Cyclic charge-discharge test.

To achieve a better understanding of whether the ion-conductive hydrogel could be served as a wearable self-powered sensor, the mechanical properties of the quasi-solid state hydrogel are investigated by using tensile machine with a 100 N load cell for tension. The ion-conductive hydrogel shows a maximum elongation more than 2800%

https://dx.doi.org/10.1016/j.nanoen.2021.106272

with a tensile rate of 100 mm min^{-1}, indicating that the resulting hydrogel had an outstanding elasticity (Fig. 4a). In order to further characterize the energy dissipation behavior and self-recovery properties of the ion-conductive hydrogel, a series of cyclic loading-unloading tests at different strains are measured as shown in Fig. 4b. Apparently, the ion-conductive hydrogel displays hysteresis loops and hysteresis loops enlarged gradually as the strain increased from 50% to 300%. In the process of hydrogel stretching, dynamic cross-linking such as hydrogen bond can effectively dissipate energy. With the increase of strain, more cross-linking points are destroyed, dissipating lots of energy and eventually leading to the increase of hysteresis loop. Besides, each loading curve overlapped with the previous one, indicating that the hydrogel has the self-recovery properties. This energy dissipation behavior and self-recovery properties are conductive to synthesis high tensile property hydrogel.

For strain sensors in wearable devices, sensitivity is significantly crucial. Generally, gauge factor ($GF= (R-R_0/R_0)/\varepsilon$) is used to represent the sensitivity, where R and R_0 are the resistances of the original and stretched hydrogels, respectively, and ε is the applied strain of the hydrogel. Fig. S5 shows the variation of GF under different strains from 0% to 2300%. The gauge factor is 3.3 (R^2=0.968) at 0-170% strain and 5.0 (R^2=0.997) at 170-460% strain. As the applied strain increases further, the gauge factor reaches 8.2, 13.5 and 9.6 in the strain range of 460-1270%, 1270-1570% and 1570-2300%, respectively. A great sensitivity is essential to detect changes in human movement.

For an ion-conducting hydrogel, the ions are dispersed in the network of the

https://dx.doi.org/10.1016/j.nanoen.2021.106272

hydrogel as conductive fillers. When a tensile strain is applied to the hydrogel, the distance between the ions enlarge, resulting in an increase in the resistance of the hydrogel. When the tension is removed, owing to various intermolecular forces, the hydrogel can be restored to the original state. The ion distance is reduced and the resistance is returned to the initial value[37]. Applying different strains will result in different ion distances, which is different resistances, and using the relative resistance change as the output signal to represent the external input signal. Fig. 4c indicates that the strain input is highly consistent with the corresponding electrical signal output, indicating that the signal hysteresis of the ion-conductive hydrogel can be ignored. Simultaneously, it is also highly consistent under different strains and within multiple cycles. Simultaneously, the influence of ambient temperature on the output signal have been excluded. As shown in Fig.S6, the output signal of the ion-conductive hydrogel at different temperatures remained consistent. In human motion, different types of motion have different stretching rates. Therefore, it is of great significance to investigate the sensitivity of strain sensors under different tensile rates. As Fig. 4d depicts, the relative resistance changes at different tensile rates (50,100 and 200 $mm \cdot min^{-1}$) and strains (50% and 100%) are investigated. The result indicates that there is a slight difference in the relative resistance change at different tensile rates. In order to ensure the normal operation of the ion-conductive hydrogel strain sensor under different small strains, tensile tests under different gradient strains have been conducted, and the results show a consistent gradient (Fig. 4e). The durability of sensor is an important indicator for wearable device. Fig. 4f depicts that the ion-conductive hydrogel shows stable output

https://dx.doi.org/10.1016/j.nanoen.2021.106272

$\Delta R/R_0$ signal during 1300 stretching and releasing cycles at a 10% strain. The good cycling stability may result from the double network and the self-recovery property of the ion-conductive hydrogel.

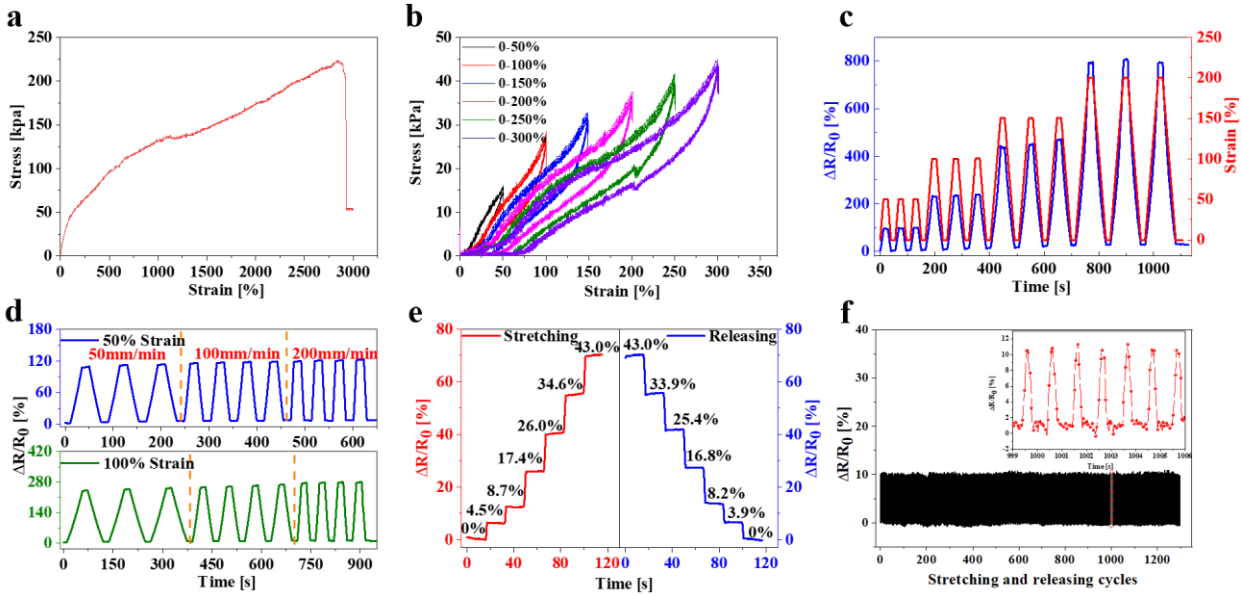

Figure 4. (a) Tensile stress-strain curves for the ion-conductive hydrogel. (b) Cyclic tensile stress-strain curves of the ion-conductive hydrogel under various strain (50%, 100%, 150%, 200%, 250%, 300%). (c) Slight electrical hysteresis of the ion-conductive hydrogel sensor. (d) Relative resistance change at different tensile rates (50mm min^{-1}, 100mm min^{-1} and 200mm min^{-1}) and different strain (50% and 100%) of the ion-conductive hydrogel sensor. (e) Instantaneous relative resistance change during stretching and releasing. (f) output signal after 1300 stretching and releasing cycles.

To further investigate the feasibility of the hydrogel strain sensor in practical situations, the ion-conductive hydrogel sensor is connected to different parts of the human body, including finger, wrist, elbow and knee. Fig. 5a depicts the $\Delta R/R_0$ of the ion-conductive hydrogel sensor increased in real time when the finger bended. And the

https://dx.doi.org/10.1016/j.nanoen.2021.106272

$\Delta R/R_0$ further increases results from the further bending. Analogously, when the ion-conductive hydrogel sensor is connected to the wrist, it can conspicuously detect the bending of the wrist. When the wrist bends down, the $\Delta R/R_0$ of the ion-conductive hydrogel increases, and then it turns back to the initial value when the wrist restores the original state (Fig. 5b). Moreover, Fig. 5c depicts the detection of elbow bending. The $\Delta R/R_0$ of the ion-conductive hydrogel shows different values when the elbow was bent at different angles. Different knee movements can also be detected when the ion-conductive hydrogel is connected to the knee (Fig. 5d). All the above detections were periodic and stable, indicating that it is feasible for the ion-conductive hydrogel sensor applying to the detection of human movement. In order to further verify the potential of the ion-conductive hydrogel as a sensor to detect human movement, the ion-conductive hydrogel sensor is connected to the throat to detect signal changes in human vocalization. To investigate the sensing performance of the sensor when be used to monitor monitoring the human body's speech signal, the ion-conductive hydrogel sensor is tightly attached to the throat When the volunteer said the letter “AFM”, the phrase “Guangdong”, the word “Sensor” and “Friday”, respectively, the $\Delta R/R_0$ of the ion-conductive hydrogel sensor showed a corresponding variation, which was notably different and repetitive (Fig. 5e and 5f). When the volunteer makes the sound, the vibration of the throat shrinks and deduced a compressive strain on the sensor, resulting in decreasing of resistant of the sensor and the $\Delta R/R_0$ shows a negative value and there have been similar report before[38]. Therefore, the sensor can clearly distinguish between different words, including English words and Chinese phrase.

https://dx.doi.org/10.1016/j.nanoen.2021.106272

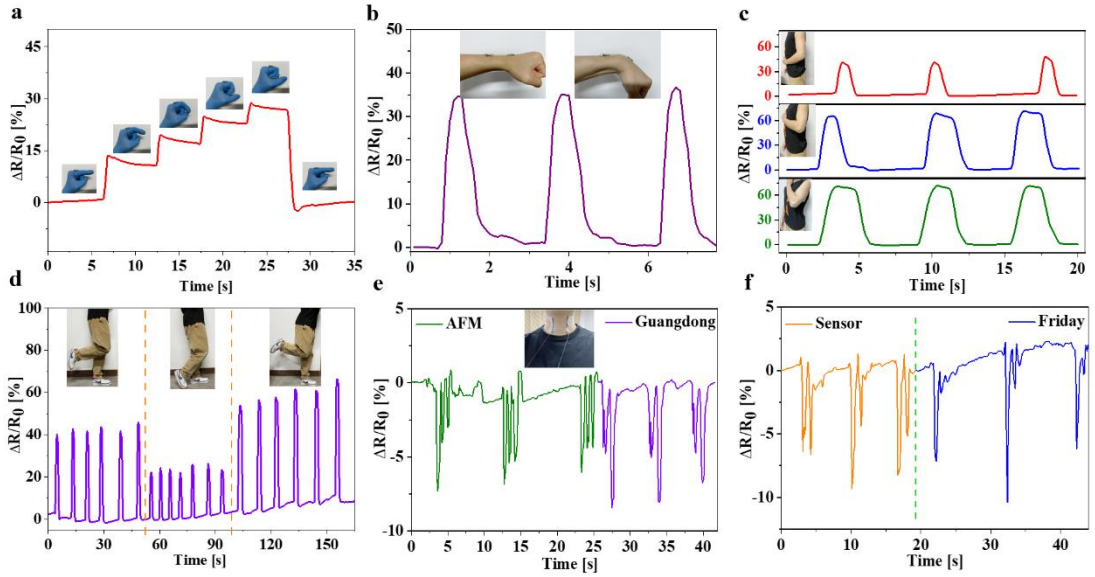

Figure 5. Real-time monitoring of human motions. (a-d) Bending of finger, wrist, elbow and knee, respectively. (e, f) Slight throat movements as the volunteer say the letter "AFM", the Chinese phrase "Guangdong", the word "Sensor" and "Friday", respectively.

In order to verify whether the ion-conductive hydrogel based thermoelectric generator can be used as a self-powered strain sensor, an external resistor R_f (10000 Ω) was selected as the load resistor which can be driven by the thermovoltage of the ion-conductive hydrogel. The structure of the self-powered ion-conductive hydrogel strain sensor is schematically illustrated in Figure 6a. According to the equation, $V_f = \frac{V_0}{R+R_f} R_f$, where V_f is the load-voltage, V_0 is the open circuit voltage of the ion-conductive hydrogel and R is the internal resistance of the ion-conductive hydrogel. When a strain is applied to the ion-conductive hydrogel at a temperature difference, the resistance change of the ion-conductive hydrogel will cause a corresponding load-voltage change of the fixed resistance if the self-powered ion-conductive hydrogel strain sensor is

https://dx.doi.org/10.1016/j.nanoen.2021.106272

achievable. Therefore, relative resistance change of the ion-conductive hydrogel can be converted into the voltage change of the fixed load resistance, thereby realizing the detection of the external input signal. As Fig.6b depicts, a stable output load-voltage of 55mV is achieved after thermal charging of the ion-conductive hydrogel. When an external pressure is applied to the ion-conductive hydrogel, the corresponding load-voltage increases and has a stable and repeatable voltage change on the fixed load resistance due to the decrease of the ion-conductive hydrogel resistance R. With the increase of external pressure, that is, the increase of compressive strain, the change of load-voltage increases. Accordingly, the relative load-voltage variations of the ion-conductive hydrogel increases with the increasing of compression strain, indicating that the external input signal can be converted into the relative load-voltage variations of the fixed load resistor (Fig.6c).

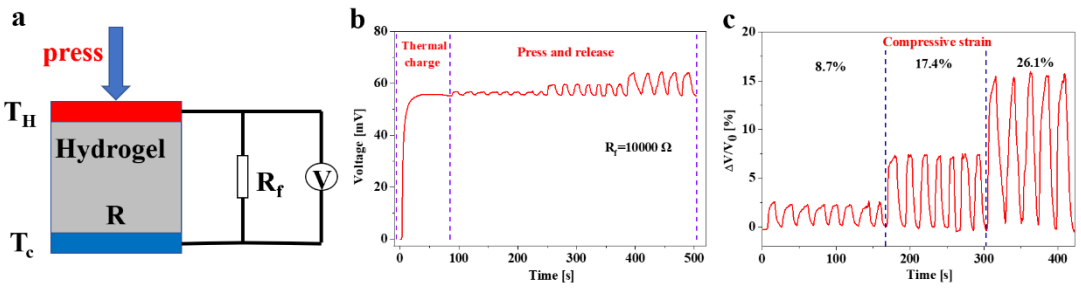

Figure 6. (a) Schematic illustration of the self-powered ion-conductive hydrogel strain sensor. (b) Thermal charge and the variation of the voltage upon pressing and relaxation for the ion-conductive hydrogel at the external resister R_f =10000 Ω and △T = 40K. (c) Relative load-voltage variations of the self-powered ion-conductive hydrogel strain sensor.

https://dx.doi.org/10.1016/j.nanoen.2021.106272

Conclusion

In summary, we have demonstrated a wearable self-powered strain sensor based on quasi-solid state hydrogel of Li_2SO_4/PAAm/CA that can harvest the human body heat to generate a thermovoltage. The as-prepared ion-conductive hydrogel sensor has a 2800% elongation at break and high sensitivity (GF=4 when the strain is 200%), which is effortless to detect the movement and sound of human body. High Seebeck efficient of 11.5 mV K^{-1} was obtained and the maximum output power density was 94.38 mW m^{-2} at a temperature difference of 40 K. In addition, the ion-conductive hydrogel has an impressive ZT value of 0.087. The ion-conductive hydrogel was able to work in quasi-continuous thermal charge-discharge, indicating that the self-powered ion-conductive hydrogel sensor is not disposable. Combining the merits of flexibility, superior sensing and thermoelectric performances at room temperature range together, we believe that the self-power sensor will render new numerous motion detections and low-grade heat harvesting applications like wearable electronics, sports, health and wellbeing.

Experimental section

Materials. Acrylamide (AAm,99%), *N, N′*-methylenebis-acrylamide (MBAA), Lithium sulphat (Li_2SO_4,99%) and N, N, N', N'-Tetramethylethylenediamine (TEMED,99%) were purchased from Macklin (Shanghai, China). Calcium chloride ($CaCl_2$), Sodium alginate (SA), Potassium persulfate (KPS) and glycerol were purchased from Aladdin (Shanghai, China).

https://dx.doi.org/10.1016/j.nanoen.2021.106272

Preparation of Li_2SO_4/PAAm/CA hydrogel. First, 2 g SA was dissolved in 198 g water and glycerol (1:1) and then stirred at room temperature until the solution became clear. 4 g AAm, 0.3 g Li_2SO_4 and 5 mg KPS were sequentially dissolved into 4.8 g the above solution and some water, and mixed it vigorously in the ice bath for half an hour. 1 mg MBAA and 50 μL TEMED were then added while stirring and ultrasonicated for 5 minutes to remove air bubbles. Finally, the resulting solution were added to a silicon mold (Cylinder structure with 15 mm high and 15mm in diameter) for natural polymerization at room temperature for 24 h to obtain Li_2SO_4/PAAm/SA hydrogel. Li_2SO_4/ PAAm/ CA hydrogel was obtained by soaking the Li_2SO_4/PAAm/SA hydrogel in 1M calcium chloride solution for some time.

Characterization and Measurement. The mechanical properties were tested by a tensile machine with a 100 N load cell at 25℃. For the strain sensing experiment, the tensile rate was 100 mm min^{-1} if there are no special instructions and the ion-conductive hydrogel was cut to 15 mm× 10 mm× 2 mm to test. The relative resistance changes ($\Delta R/R_0$) of the ion-conductive hydrogel were measured by the electrochemical workstation (Chi660e). Thermoelectric effects were measured using a temperature controller and the same electrochemical workstation. Thermal conductivity was measured by the transient plane heat source method (TPS2500S, Sweden). The ionic conductivity was measured by AC impedance spectroscopy (Chi660e). The Seebeck coefficient was obtained from the slope of the fitting line of the thermal voltage at

https://dx.doi.org/10.1016/j.nanoen.2021.106272

different temperature differences. The ZT value was calculated by the following formula: $ZT = \frac{\sigma \alpha^2}{\lambda} T$, where T, λ, σ, and α are the absolute temperature, thermal conductivity, ionic conductivity, and Seebeck coefficient, respectively.

Acknowledgements

The work has been partially supported by National Natural Science Foundation of China (Grant No. 52073066, 21673080) and the GDAS Project of Science and Technology Development（Grant No. 2020GDASYL-20200102028).

References

[1] W. Zeng, L. Shu, Q. Li, S. Chen, F. Wang, X.-M. Tao, Fiber-Based Wearable Electronics: A Review of Materials, Fabrication, Devices, and Applications, Advanced Materials 26(31) (2014) 5310-5336.

[2] X. Wang, Y. Gu, Z. Xiong, Z. Cui, T. Zhang, Silk-Molded Flexible, Ultrasensitive, and Highly Stable Electronic Skin for Monitoring Human Physiological Signals, Advanced Materials 26(9) (2014) 1336-1342.

[3] J.-Y. Sun, C. Keplinger, G.M. Whitesides, Z. Suo, Ionic Skin, Advanced Materials 26(45) (2014) 7608-7614.

[4] Y. Zang, F. Zhang, C.-a. Di, D. Zhu, Advances of flexible pressure sensors toward artificial intelligence and health care applications, Materials Horizons 2(2) (2015) 140-156.

[5] T. Tran Quang, N.-E. Lee, Flexible and Stretchable Physical Sensor Integrated

https://dx.doi.org/10.1016/j.nanoen.2021.106272

Platforms for Wearable Human-Activity Monitoring and Personal Healthcare, Advanced Materials 28(22) (2016) 4338-4372.

[6] G. Cai, J. Wang, K. Qian, J. Chen, S. Li, P.S. Lee, Extremely Stretchable Strain Sensors Based on Conductive Self-Healing Dynamic Cross-Links Hydrogels for Human-Motion Detection, Advanced Science 4(2) (2017).

[7] S. Xia, S. Song, G. Gao, Robust and flexible strain sensors based on dual physically cross-linked double network hydrogels for monitoring human-motion, Chemical Engineering Journal 354 (2018) 817-824.

[8] X. Sun, Z. Qin, L. Ye, H. Zhang, Q. Yu, X. Wu, J. Li, F. Yao, Carbon nanotubes reinforced hydrogel as flexible strain sensor with high stretchability and mechanically toughness, Chemical Engineering Journal 382 (2020).

[9] Y. Cai, J. Qin, W. Li, A. Tyagi, Z. Liu, M.D. Hossain, H. Chen, J.-K. Kim, H. Liu, M. Zhuang, J. You, F. Xu, X. Lu, D. Sun, Z. Luo, A stretchable, conformable, and biocompatible graphene strain sensor based on a structured hydrogel for clinical application, Journal of Materials Chemistry A 7(47) (2019) 27099-27109.

[10] L.E. Kreno, K. Leong, O.K. Farha, M. Allendorf, R.P. Van Duyne, J.T. Hupp, Metal-Organic Framework Materials as Chemical Sensors, Chemical Reviews 112(2) (2012) 1105-1125.

[11] P.-Y. Du, S.-Y. Liao, W. Gu, X. Liu, A multifunctional chemical sensor based on a three-dimensional lanthanide metal-organic framework, Journal of Solid State Chemistry 244 (2016) 31-34.

[12] F.-Y. Yi, D. Chen, M.-K. Wu, L. Han, H.-L. Jiang, Chemical Sensors Based on

https://dx.doi.org/10.1016/j.nanoen.2021.106272

Metal-Organic Frameworks, Chempluschem 81(8) (2016) 675-690.

[13] C. Baratto, G. Faglia, G. Sberveglieri, Z. Gaburro, L. Pancheri, C. Oton, L. Pavesi, Multiparametric porous silicon sensors, Sensors 2(3) (2002) 121-126.

[14] Z. Gaburro, L. Pavesi, C. Baratto, G. Faglia, G. Sberveglieri, A porous silicon microcavity as an optical and electrical multipatrametric chemical sensor, in: E.V. Buzaneva, P. Scharff (Eds.), Frontiers of Multifunctional Nanosystems2002, pp. 399-412.

[15] E. Comini, C. Baratto, G. Faglia, M. Ferroni, A. Vomiero, G. Sberveglieri, Quasi-one dimensional metal oxide semiconductors: Preparation, characterization and application as chemical sensors, Progress in Materials Science 54(1) (2009) 1-67.

[16] Y. Wang, W. Zhu, Y. Deng, B. Fu, P. Zhu, Y. Yu, J. Li, J. Guo, Self-powered wearable pressure sensing system for continuous healthcare monitoring enabled by flexible thin-film thermoelectric generator, Nano Energy 73 (2020).

[17] D.Y. Park, D.J. Joe, D.H. Kim, H. Park, J.H. Han, C.K. Jeong, H. Park, J.G. Park, B. Joung, K.J. Lee, Self-Powered Real-Time Arterial Pulse Monitoring Using Ultrathin Epidermal Piezoelectric Sensors, Adv Mater 29(37) (2017).

[18] F.R. Fan, W. Tang, Z.L. Wang, Flexible Nanogenerators for Energy Harvesting and Self-Powered Electronics, Advanced Materials 28(22) (2016) 4283-4305.

[19] L. Lin, Y. Hu, C. Xu, Y. Zhang, R. Zhang, X. Wen, Z.L. Wang, Transparent flexible nanogenerator as self-powered sensor for transportation monitoring, Nano Energy 2(1) (2013) 75-81.

[20] S. Wang, L. Lin, Z.L. Wang, Triboelectric nanogenerators as self-powered active

https://dx.doi.org/10.1016/j.nanoen.2021.106272

sensors, Nano Energy 11 (2015) 436-462.

[21] Z.L. Wang, Triboelectric Nanogenerators as New Energy Technology for Self-Powered Systems and as Active Mechanical and Chemical Sensors, Acs Nano 7(11) (2013) 9533-9557.

[22] Z. Liu, S. Zhang, Y.M. Jin, H. Ouyang, Y. Zou, X.X. Wang, L.X. Xie, Z. Li, Flexible piezoelectric nanogenerator in wearable self-powered active sensor for respiration and healthcare monitoring, Semiconductor Science and Technology 32(6) (2017).

[23] S. Siddiqui, D.-I. Kim, E. Roh, D. Le Thai, T. Tran Quang, N. Minh Triet, N.-E. Lee, A durable and stable piezoelectric nanogenerator with nanocomposite nanofibers. embedded in an elastomer under high loading for a self-powered sensor system, Nano Energy 30 (2016) 434-442.

[24] B.J. Kim, D.H. Kim, Y.-Y. Lee, H.-W. Shin, G.S. Han, J.S. Hong, K. Mahmood, T.K. Ahn, Y.-C. Joo, K.S. Hong, N.-G. Park, S. Lee, H.S. Jung, Highly efficient and bending durable perovskite solar cells: toward a wearable power source, Energy & Environmental Science 8(3) (2015) 916-921.

[25] M.R. Burton, S. Mehraban, D. Beynon, J. McGettrick, T. Watson, N.P. Lavery, M.J. Carnie, 3D Printed SnSe Thermoelectric Generators with High Figure of Merit, Advanced Energy Materials 9(26) (2019).

[26] G. Hu, H. Edwards, M. Lee, Silicon integrated circuit thermoelectric generators with a high specific power generation capacity, Nature Electronics 2(7) (2019) 300-306.

[27] X. Zhang, N. Sheng, L. Wang, Y. Tan, C. Liu, Y. Xia, Z. Nie, K. Sui,

https://dx.doi.org/10.1016/j.nanoen.2021.106272

Supramolecular nanofibrillar hydrogels as highly stretchable, elastic and sensitive ionic sensors, Materials Horizons 6(2) (2019) 326-333.

[28] S. Han, C. Liu, X. Lin, J. Zheng, J. Wu, C. Liu, Dual Conductive Network Hydrogel for a Highly Conductive, Self-Healing, Anti-Freezing, and Non-Drying Strain Sensor, ACS Applied Polymer Materials 2(2) (2020) 996-1005.

[29] Y.-Z. Zhang, K.H. Lee, D.H. Anjum, R. Sougrat, Q. Jiang, H. Kim, H.N. Alshareefit, MXenes stretch hydrogel sensor performance to new limits, Science Advances 4(6) (2018).

[30] D. Zhao, H. Wang, Z.U. Khan, J.C. Chen, R. Gabrielsson, M.P. Jonsson, M. Berggren, X. Crispin, Ionic thermoelectric supercapacitors, Energy & Environmental Science 9(4) (2016) 1450-1457.

[31] J. Duan, G. Feng, B. Yu, J. Li, M. Chen, P. Yang, J. Feng, K. Liu, J. Zhou, Aqueous thermogalvanic cells with a high Seebeck coefficient for low-grade heat harvest, Nat Commun 9(1) (2018) 5146.

[32] H. Cheng, X. He, Z. Fan, J. Ouyang, Flexible Quasi-Solid State Ionogels with Remarkable Seebeck Coefficient and High Thermoelectric Properties, Advanced Energy Materials 9(32) (2019).

[33] H. Gao, B. Guo, J. Song, K. Park, J.B. Goodenough, A Composite Gel-Polymer/Glass-Fiber Electrolyte for Sodium-Ion Batteries, Advanced Energy Materials 5(9) (2015).

[34] M.S. Dresselhaus, G. Chen, M.Y. Tang, R.G. Yang, H. Lee, D.Z. Wang, Z.F. Ren, J.P. Fleurial, P. Gogna, New directions for low-dimensional thermoelectric materials,

https://dx.doi.org/10.1016/j.nanoen.2021.106272

Advanced Materials 19(8) (2007) 1043-1053.

[35] B. Luo, D. Ye, L. Wang, Recent Progress on Integrated Energy Conversion and Storage Systems, Advanced Science 4(9) (2017).

[36] C.-G. Han, X. Qian, Q. Li, B. Deng, Y. Zhu, Z. Han, W. Zhang, W. Wang, S.-P. Feng, G. Chen, W. Liu, Giant thermopower of ionic gelatin near room temperature, Science 368(6495) (2020) 1091-+.

[37] X. Sun, F.L. Yao, J.J. Li, Nanocomposite hydrogel-based strain and pressure sensors: a review, Journal of Materials Chemistry A 8(36) (2020) 18605-18623.

[38] G. Ge, Y. Lu, X. Qu, W. Zhao, Y. Ren, W. Wang, Q. Wang, W. Huang, X. Dong, Muscle-Inspired Self-Healing Hydrogels for Strain and Temperature Sensor, Acs Nano 14(1) (2020) 218-228.

https://dx.doi.org/10.1016/j.nanoen.2021.106272

Declaration of interests

The authors declare that they have no known competing financial interests or personal relationships that could have appeared to influence the work reported in this paper.